

GENERAL ANALYTIC SOLUTION OF THE WAVE EQUATION FOR ANISOTROPIC MATERIALS USING SYMBOLIC MANIPULATION

R. B. Mignogna
Mechanics of Materials Branch
Naval Research Laboratory
Washington, DC 20375-5000

INTRODUCTION

Almost all solutions for elastic waves in anisotropic materials have been obtained by approximation methods [1], numerical techniques [2], or in special symmetry [3, 4] directions where factored solutions can be obtained. Even for special symmetry directions, the analysis becomes quite laborious for lower symmetry classes.

It is interesting to note that the method by which one could obtain a general closed form solution for the wave equation has been readily available since the 16th century. That method is to use the general solution for a cubic equation, sometimes referred to as Cardanos formula.

Every [5] followed a similar approach, using the trigonometric solution for the cubic equation, and obtained a general closed-form solution for the wave equation. The differences in the current work is the utilization of one of the newer computer tools available, symbolic manipulation and the approach permitted by this tool. The computer/software will be referred to as the machine.

The purpose of this paper is to present a very straight forward approach and indicate the utility, advantages and power of using symbolic manipulation to obtain a general closed-form analytic solution for bulk waves in anisotropic materials. A mapping will be presented for easy comparison of entire three dimensional velocity or slowness surfaces. Also some differences between the general solution and those obtained by considering special symmetry directions will be discussed. Velocity, slowness and wave surfaces are shown for materials that can be easily compared in the literature [3, 4]. The values for density and elastic constants used are from the literature [3, 4].

GENERAL SOLUTION

The equation of motion for a bulk wave in an unbounded material may be expressed as

$$C_{ijkl} \left(\frac{\partial^2 u_k}{\partial x_i \partial x_j} \right) = \rho \ddot{u}_i \quad (1)$$

where C_{ijkl} are the elastic constants, u_i are the particle displacements and ρ the density. Assuming a plane wave of the form $u_i = A_i^o \exp i(kn_r x_r - \omega t)$ and substituting into the equation of motion, Christoffels equation may be obtained $(\Gamma_{ik} - \rho v^2 \delta_{ik})u_k = 0$ where δ_{ik} is the Kroneker

delta and the Christoffels stiffnesses, Γ_{ik} are $\bar{\Gamma} = \Gamma_{ik} = C_{ijkl}n_j n_l$ being the direction cosines. For non-zero displacements we must have

$$\det(\Gamma_{ik} - \rho v^2 \delta_{ik}) = 0. \quad (2)$$

Substituting V for ρv^2 , and evaluating the determinant we have

$$V^3 - tr(\bar{\Gamma})V^2 + tr_2(\bar{\Gamma})V + |\bar{\Gamma}| = 0 \quad (3)$$

i.e., the characteristic polynomial. The $tr_2(\bar{\Gamma})$ is the trace of the matrix of minor determinants of $\bar{\Gamma}$. By substituting a_1, a_2 , and a_3 for $-tr(\bar{\Gamma}), tr_2(\bar{\Gamma})$ and $|\bar{\Gamma}|$ respectively, we have a general cubic equation.

All that has been presented to this point can be done by hand or by machine with equal ease if Christoffel stiffnesses are not expanded. Those having access to symbolic computation have a distinct advantage in their efficiency. At this point the machine should be able to obtain the roots of the cubic equation in closed form.

To do so by hand, one could follow the method of Cardano and use the substitution $V = Y - a_1/3$ to eliminate the squared term yielding

$$Y^3 + b_1 Y + b_2 = 0 \quad (4)$$

where $b_1 = (3a_2 - a_1^2)/3$ and $b_2 = (2a_1^3 - 9a_1 a_2 + 27a_3)/27$. The solution for a cubic equation of this form may be found in [6, 7, and 8]. From [7]

$$Y_1 = D_1 + D_2$$

$$Y_2 = \frac{-(D_1 + D_2)}{2} + \frac{(D_1 - D_2)i\sqrt{3}}{2} \quad (5)$$

$$Y_3 = \frac{-(D_1 + D_2)}{2} - \frac{(D_1 - D_2)i\sqrt{3}}{2}$$

where $D_1 = \left[\frac{-b_2}{2} + \sqrt{\frac{b_2^2}{4} + \frac{b_1^3}{27}} \right]^{\frac{1}{3}}$ and $D_2 = \left[\frac{-b_2}{2} - \sqrt{\frac{b_2^2}{4} + \frac{b_1^3}{27}} \right]^{\frac{1}{3}}$. Since we are looking for free bulk waves, we desire only real solutions and must have

$$\left[\frac{b_2^2}{4} + \frac{b_1^3}{27} \right] \leq 0 \quad (6)$$

Setting

$$d_1 = \frac{-b_2}{2} \quad \text{and} \quad d_2 = \sqrt{-\left[\frac{b_2^2}{4} + \frac{b_1^3}{27} \right]} \geq 0 \quad \text{i.e.} \quad D_1 = (d_1 + id_2)^{\frac{1}{3}} \quad (7)$$

one can substitute (7) into D_1 and D_2 and use DeMoivre's theorem to obtain

$$D_1 + D_2 = 2(d_1^2 + d_2^2)^{\frac{1}{6}} \cos \left[\frac{(\tan^{-1} d_2/d_1)}{3} \right]$$

$$i(D_1 - D_2) = 2(d_1^2 + d_2^2)^{\frac{1}{6}} \sin \left[\frac{(\tan^{-1} d_2/d_1)}{3} \right] \quad (8)$$

If we let $r = (d_1^2 + d_2^2)$ and $\gamma = \tan^{-1}d_2/d_1$, combine the sine and cosine terms and perform all the necessary substitutions, for any symmetry class, the general solutions (real) for the phase velocity can be written as

$$\begin{aligned} \rho v_1^2 &= 2r^{\frac{1}{6}} \cos \left[\frac{\gamma}{3} \right] - \frac{a_1}{3} \\ \rho v_2^2 &= 2r^{\frac{1}{6}} \cos \left[\gamma_3 + \tan^{-1}\sqrt{3} \right] - \frac{a_1}{3} \\ \rho v_3^2 &= 2r^{\frac{1}{6}} \cos \left[\gamma_3 - \tan^{-1}\sqrt{3} \right] - \frac{a_1}{3}. \end{aligned} \tag{9}$$

The roots, for (4), obtained by the machine are the same as (5) but may have terms grouped in a different manner, such as

$$\begin{aligned} Y_1 &= D_1 - b_1/3D_1 \\ Y_2 &= \left[-\frac{i\sqrt{3}}{2} - \frac{1}{2} \right] D_1 - \left[\frac{i\sqrt{3}}{2} - \frac{1}{2} \right] \frac{b_1}{3D_1} \\ Y_3 &= \left[\frac{i\sqrt{3}}{2} - \frac{1}{2} \right] D_1 - \left[-\frac{i\sqrt{3}}{2} - \frac{1}{2} \right] \frac{b_1}{3D_1} \end{aligned} \tag{10}$$

By making a substitution in the roots obtained by the machine for the terms that appear in D_1 , under the square root, i.e., (id_2), similar to that shown above, the solution can easily be restricted to real values by using the machine to take the "real parts."

Having obtained a closed form solution for the phase velocity, the ray or group (energy) velocity (for certain cases) and the eigenvectors may also be expressed in an analytic closed form. As shown by Federov [9] and Every [5], the ray velocity can be written as

$$E_j = \partial\omega/\partial k_j \tag{11}$$

Substituting $\omega = k v$ into (11), the components of the ray velocity can be expressed as a function of the phase velocity as

$$E_j = \partial v / \partial n_j \tag{12}$$

Using the results of Musgrave [10], the components of the eigenvector as a function of the phase velocity are

$$A_1^o = \frac{\alpha}{A_1 A}, \quad A_2^o = \frac{\beta}{A_2 A}, \quad A_3^o = \frac{\gamma}{A_3 A} \tag{13}$$

where $\alpha = \left(\frac{\Gamma_{12}\Gamma_{13}}{\Gamma_{23}} \right)^{\frac{1}{2}}, \beta = \left(\frac{\Gamma_{12}\Gamma_{23}}{\Gamma_{13}} \right)^{\frac{1}{2}}, \gamma = \left(\frac{\Gamma_{13}\Gamma_{23}}{\Gamma_{12}} \right)^{\frac{1}{2}},$

$$A = \left[\frac{\alpha^2}{A_1^2} + \frac{\beta^2}{A_2^2} + \frac{\gamma^2}{A_3^2} \right]^{\frac{1}{2}} \quad \text{and} \quad A_i = \rho v^2 - \Gamma_{ii} + \alpha^2.$$

“PRE” AND “POST-SIMPLIFICATION” OF THE CHARACTERISTIC POLYNOMIAL

For certain symmetry planes, if the Christoffel stiffnesses are simplified before solving for the roots of the characteristic polynomial (“pre-simplification”), the resulting polynomial can be readily factored. As an example, the resulting polynomial for the (110) symmetry plane in cubic material can be factored into one “pure” root with the other two roots obtained by the quadratic equation. Although both solution sets must agree, when the general solution is obtained for the characteristic polynomial and then simplified for the (110) plane (“post-simplification”), the “grouping” of the solution set is different from the “pre-simplified” case. This difference is shown in Figs. 1 and 2 for the (110) plane in iron. The general solution gives three separable velocity surfaces, regardless of mode, i.e. pure-longitudinal, quasi-longitudinal, quasi-shear or pure shear. The disregard of mode is especially evident for tellurium dioxide, discussed later.

UTILITY OF SYMBOLIC MANIPULATION

Even for cubic materials where the high degree of symmetry greatly reduces the amount of effort needed to obtain solutions for particular symmetry planes such as the (110) plane shown in Fig. 1, the effort is tedious. Planes of less symmetry, even for cubic materials, may not be readily “factorable” and require the use of the “general solution.” The effort required to use the general solution should be obvious to those who have worked through any symmetry plane.

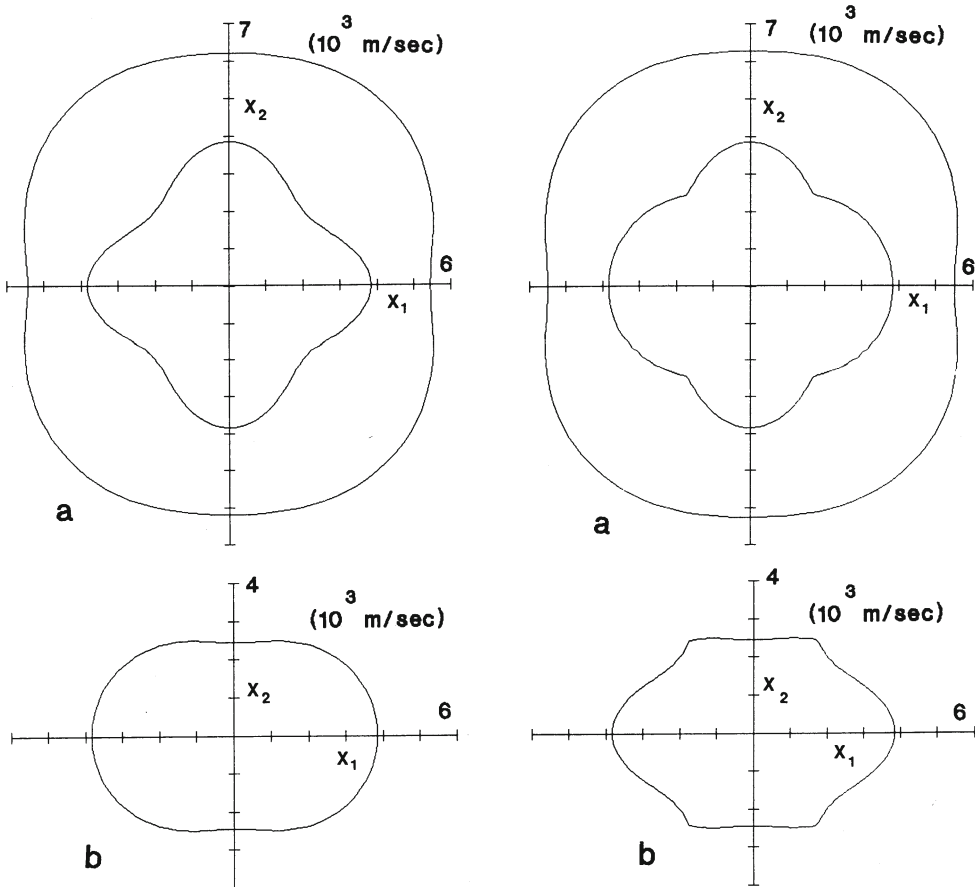


Fig. 1 — Velocity surfaces in iron (110) plane, “factored” case. Fig. 2 — Velocity surfaces in iron (110) plane, general solution.

Obtaining the general solution by symbolic manipulation has been described earlier. Once the solution is in the machine, procedures for obtaining velocity surfaces in any plane are straight forward substitutions and can be obtained in a few minutes. Examples are shown in Fig. 3 for the iron (111), (112), and (345) planes. The (111), (112), and (345) planes exhibit decreasing degrees of symmetry, three-fold, two-fold and mirror plane, respectively. The (345) plane was chosen as an example of an "arbitrary" plane.

Three dimensional velocity surfaces can be obtained just as easily as the velocity surfaces in a plane. The general solution produces three separable velocity surfaces. Attempting to graphically display the three surfaces simultaneously in a three dimensional cartesian coordinate system requires "looking" through the outer surfaces to see the inner ones. Although, this is a more conceptually appealing form, as it is easy to visualize in the mind and relate to the crystal structure, a mapping of the polar angles into a plane permits the comparison of the velocity surfaces to each other. This mapping also allows easier visualization of particular features of the velocity surfaces. Figure 4 presents the mapping schematically. The direction of the phase velocity is

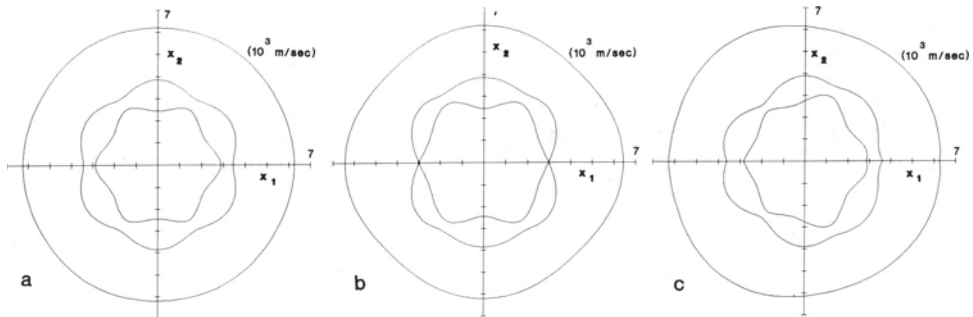


Fig. 3 — Velocity surfaces for iron calculated with general solution: (a) (111) plane, (b) (112) plane, and (c) (345) plane.

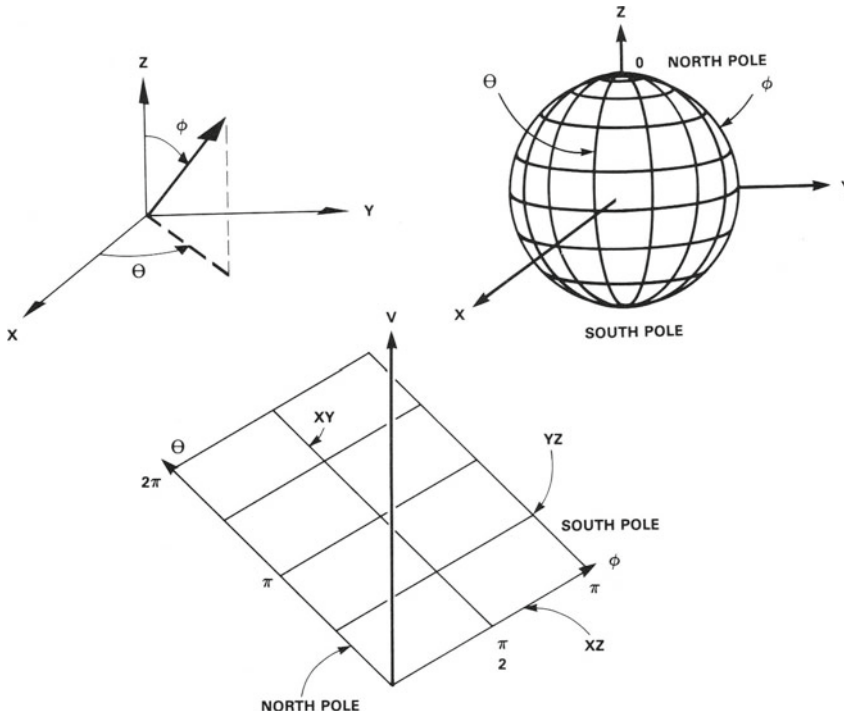


Fig. 4 — Schematic diagram showing mapping of velocity surfaces.

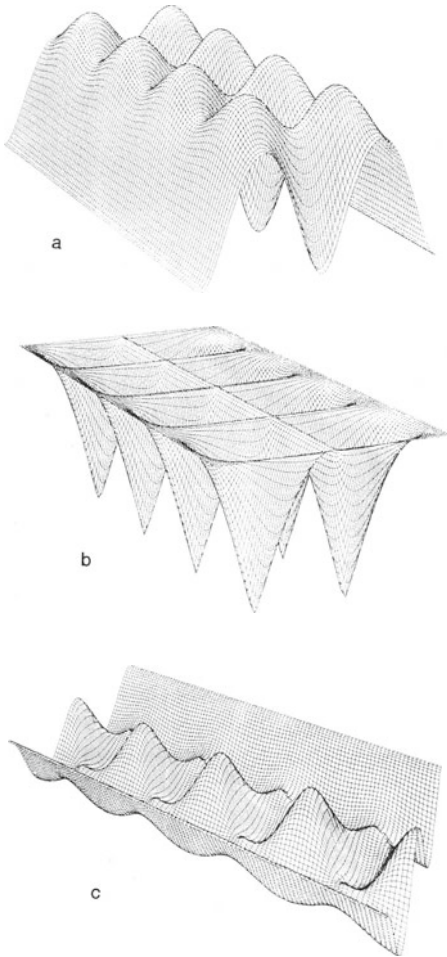


Fig. 5 — Three dimensional velocity surfaces for iron, maximum and minimum velocities (10^3 m/sec) for each surface are, respectively: (a) 6.43 and 5.44, (b) 3.85 and 2.99, and (c) 3.84 and 2.44.

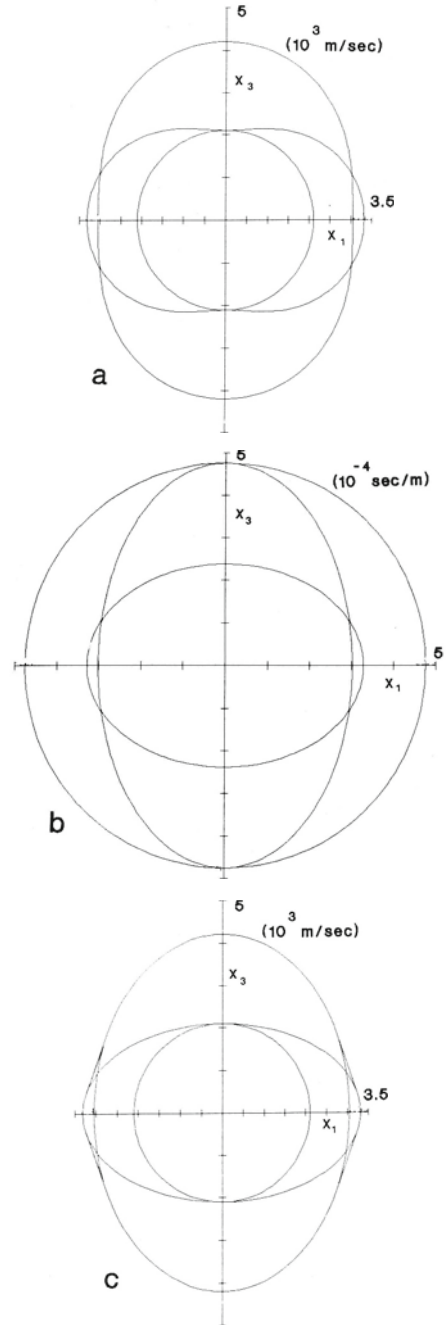
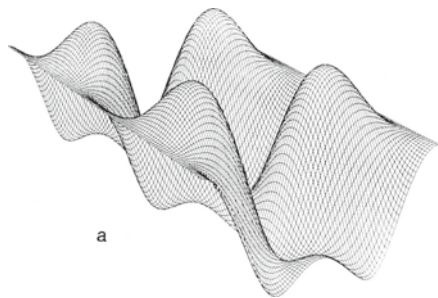
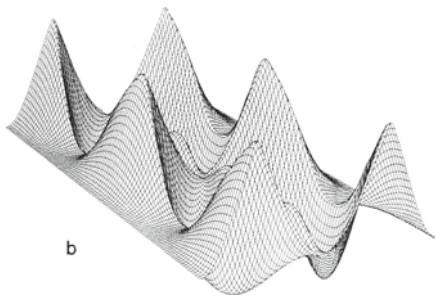


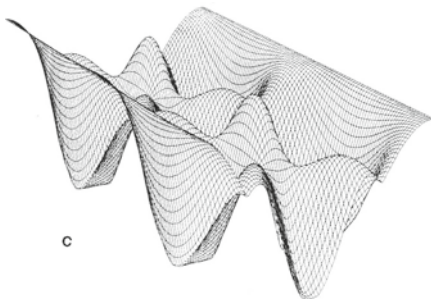
Fig. 6 — Tellurium dioxide (010) plane: (a) velocity surface, (b) slowness surface, and (c) wave surface.



a

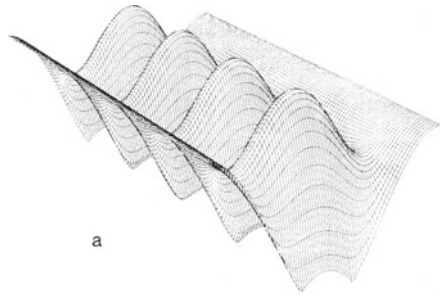


b

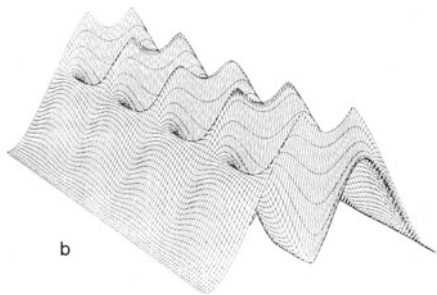


c

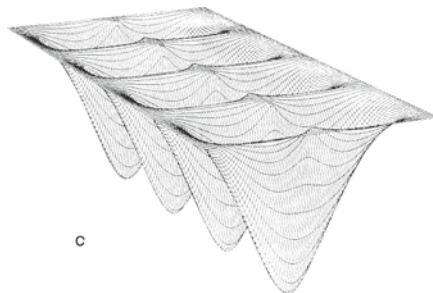
Fig. 7 — Three dimensional velocity surfaces for tellurium dioxide, maximum and minimum velocities (10^3 m/sec) for each surface are, respectively: (a) 4.46 and 3.21, (b) 3.19 and 2.10, and (c) 2.10 and 0.61.



a



b



c

Fig. 8 — Three dimensional velocity surfaces for uranium, maximum and minimum velocities (10^3 m/sec) for each surface are, respectively: (a) 3.96 and 3.22, (b) 2.55 and 1.96, and (c) 2.33 and 1.78.

described by the polar angles θ and ϕ , where $0 < \theta < 2\pi$ and $0 < \phi < \pi$. These angles are then mapped to a plane and the magnitude of the velocity becomes the "z" axis, as shown in Fig. 4. It should be noted that the points labelled "north" and "south" pole are mapped to a lines.

Using the mapping just described, the entire three dimensional velocity surfaces for iron (cubic) are presented in Fig. 5. The general solution was used in the calculations. The surfaces are not equally scaled. The maximum and minimum velocity for each surface is given in the figure captions. An interesting feature should be noted in Fig. 5, the six tips of the downward-pointing "cones" of Fig. 5b intersect the six, small, upward-pointing cones of Fig. 5c. These points represent shear waves in the (111)-type directions and are degenerate. The cones of Fig. 5c tend to "wash out" when using a three-dimensional cartesian representation, but they are prominent features using this type of display.

As mentioned previously, the general solution gives three separable velocity surfaces, regardless of mode. Tellurium dioxide is tetragonal and has the interesting property that $C_{66} > C_{11}$. In this material, for particular directions, one of the shear waves is actually faster than the longitudinal wave. The velocity, slowness and wave surfaces for the (010) plane in tellurium dioxide are shown in Fig. 6, (calculated using the general solution as are all of the later figures). When calculated by "pre-simplification," the three slowness surfaces for the (010) plane in tellurium dioxide are smooth ellipses. The general solution (Fig. 6b) again separates into fast, slow and "in between" surfaces, similar to that shown in Fig. 2. The inner curve of the slowness surfaces becomes a truncated ellipse having both longitudinal and shear modes on the same curve. This is not evident when all three curves are displayed on the same set of axes. Except for the "grouping" of the solution sets, all is in agreement with slowness surface shown by Auld [4].

Figure 7 presents the full three dimensional velocity surfaces for tellurium dioxide. It should be noted that each of the two faster surfaces, Fig. 7a and b, contain both longitudinal and shear modes. As a further example of the utility of symbolic manipulation with the general solution, the full three dimensional velocity surfaces for uranium are shown in Fig. 8. The interest in presenting uranium is due to its orthorhombic symmetry and previous treatment by Musgrave [3].

CONCLUSIONS

A very straight forward approach has been presented for the general closed-form solution for elastic bulk waves. The utility of symbolic manipulation as a tool for obtaining and rapidly using the general solution has, hopefully, been demonstrated. A mapping technique has also been presented for displaying three dimensional velocity (or slowness) surfaces for easy visual comparison.

ACKNOWLEDGMENT

The author would like to thank Dr. P. Mast and Mr. H. Chaskelis for many fruitful discussions. This work was conducted at the Naval Research Laboratory under sponsorship of the Office of Naval Research. A Symbolic 3620 computer and Macsyma was used in this work.

REFERENCES

1. J.R. Neighbours and G.E. Schacher, *J. Appl. Phys.* **38**, 5366 (1967)
2. T. Hinton and R.E. Green, Jr., *Trans. Met. Soc. AIME* **236**, 439 (1966).
3. M.J.P. Musgrave, *Crystal Acoustics* (Holden-Day, San Francisco, 1970).
4. B.A. Auld, *Acoustic Fields and Waves in Solids*, Vol. 1 (Wiley, New York, 1973).
5. A.G. Every, *Phys. Rev. B* **22**, 1746 (1980).
6. M. Richardson, *College Algebra* (Prentice-Hall, New York, 1947).
7. S.M. Selby (ed.), *CRC Standard Mathematical Tables*, 18th edition (The Chemical Rubber Co., Cleveland, 1970).
8. H.L. Pearson, *Handbook of Applied Mathematics*, edited by C.E. Pearson (Van Nostrand Reinhold Co., New York, 1974) p. 13.
9. F.I. Fedorov, *Theory of Elastic Waves in Crystals* (Plenum, New York 1968).
10. M.J.P. Musgrave, *Proc. Roy. Soc.*, A **226** (1954).